

We are IntechOpen, the world's leading publisher of Open Access books Built by scientists, for scientists

4,800

Open access books available

122,000

International authors and editors

135M

Downloads

Our authors are among the

154

Countries delivered to

TOP 1%

most cited scientists

12.2%

Contributors from top 500 universities



WEB OF SCIENCE™

Selection of our books indexed in the Book Citation Index
in Web of Science™ Core Collection (BKCI)

Interested in publishing with us?
Contact book.department@intechopen.com

Numbers displayed above are based on latest data collected.
For more information visit www.intechopen.com



Finite Element Analysis of Stationary Magnetic Field

Elena Otilia Virjoghe, Diana Enescu, Mihail-Florin Stan and Marcel Ionel

Additional information is available at the end of the chapter

<http://dx.doi.org/10.5772/50846>

1. Introduction

Computer-aided analysis of field distribution for evaluating electromagnetic device or component performance has become the most advantageous way of design. Analytical methods have limited uses and experimental methods are time intensive and expensive (Morozionkov et al., 2008).

The problems of magnetic fields calculation are aimed at determining the value of one or more unknown functions for the field considered, such as magnetic field intensity, magnetic flux density, magnetic scalar potential and magnetic vector potential. As the field has infinite points, the function values are in infinite number.

Physical phenomena of electromagnetic nature are described by Maxwell's equations from the mathematical point of view. These are differential equations with the given boundary conditions. By means of them, the exact solution of the problem is obtained. In this way, the value of function or functions in any point of the studied range is calculated. This represents the analytical way for solving the problems.

Analytical methods (conformable representation method, method of separation of the variables, Green function method) are applied to solve relatively simple problems. Problems which occur in practice are often complex concerning the geometric construction, material heterogeneity, loading conditions, boundary conditions, so that the integration of differential equations is difficult or sometimes impossible. In this case, the analytical solution can be carried out only by creating a simplified model so that the integration of differential equations is possible. Therefore, an exact solution for a simplified model can be obtained (Gârbea, 1990).

It is sometimes preferable to obtain, instead of the exact solution of the simplified model, an approximate solution of the real problem. Approximate solutions which are obtained by numerical methods reflect better the reality than exact solutions of a simplified model.

The software package ANSYS can be used for investigation of the magnetic field distribution (the magnetic flux density, the magnetic field intensity and the magnetic vector potential) and basic electromagnetic characteristics (inductance and electromagnetic force). A typical magnetic field problem is described by defining the geometry, material properties, currents, boundary conditions, and the field system equations. The computer requires the input data, the numerical solution of the field equation and output of desired parameters. If the values are found unsatisfactory, the design modified and parameters are recalculated. The process is repeated until optimum values for the design parameters are obtained.

The ANSYS program is based on the finite element method (FEM) for solving Maxwell's equations and can be used for electromagnetic field modeling, where the field is electrostatics, magnetostatics, eddy currents, time-invariant or time-harmonic and permanent magnets (ANSYS Documentation).

The finite elements method assures sufficient accuracy of electromagnetic field computation and very good flexibility when geometry is modeled and field sources are loaded.

2. The fundamental relations of the stationary magnetic field

In this section, we discuss the particular forms of the electromagnetic field theory laws for the magnetic stationary field. We consider the models of the magnetic induction versus magnetic field intensity ($B-H$) relation, passing conditions through discontinuity surfaces, the enunciation of stationary magnetic field (the sources of the field, boundary conditions), the enunciation of scalar magnetic potential - magnetostatic field problems (Dirichlet conditions, Neumann conditions) and the enunciations using the magnetic vector potential (stationary magnetic field problems). The general formulation of the uniqueness conditions gets particular forms, adapted to some geometrical configurations (plane-parallel fields, with rotation symmetry, etc.).

Depending on the relation between the magnetic induction and the intensity of the magnetic field, a few types of materials are distinguished, the most important being linear and isotropic materials, linear and non-isotropic materials, linear and non-isotropic materials, non-linear and isotropic materials, without permanent magnetization, non-linear and non-isotropic materials, materials with hysteresis.

Non-linear and isotropic materials, without permanent magnetization, are ferromagnetic materials, which are frequently used in the production of electric equipment.

2.1. Particular forms of the electromagnetic field theory laws for the stationary magnetic field

The stationary magnetic field is established by non-moving, permanently magnetized bodies and by non-moving connecting wires crossed by direct current (Mocanu, 1981). Fundamental magnetic field relationships result by customizing the general laws and material laws of the electromagnetic field in the following conditions: bodies are non-

moving $\vec{v} = 0$ and the electric and magnetic quantities are invariable in time, $\frac{\partial(\cdot)}{\partial t} = 0$. A stationary magnetic field in a conducting domain satisfies the following system of equations:

- the magnetic circuit law (Ampère's theorem)

$$\text{rot } \vec{H} = \vec{J} \quad (1)$$

- the magnetic flux law (local form)

$$\text{div } \vec{B} = 0 \quad (2)$$

- the connection law in magnetic field

$$\vec{B} = \mu_0 (\vec{H} + \vec{M}) \quad (3)$$

- the temporary magnetization law

$$\vec{M}_t = \vec{M}_t(\vec{H}). \quad (4)$$

Here, \vec{H} is the magnetic field intensity, \vec{J} is the total current density, \vec{B} is the magnetic induction, quantity \vec{M}_t is called the temporary magnetization of the material and $\mu_0 = 4\pi \cdot 10^{-7} \text{ [H} \cdot \text{m}^{-1}]$ is the vacuum permeability.

Magnetostatics is the branch in electromagnetism that studies the stationary magnetic states that do not accompany the conduction electric currents. This magnetic field is produced by permanent magnets ($\vec{J} = 0$; $\vec{v} = 0$).

2.2. Models for the B-H relation

Depending on the relation between the magnetic induction \vec{B} and the magnetic field intensity \vec{H} , a few types of materials are distinguished (Andrei et al. 2012).

2.2.1. Linear and isotropic materials

The most important type of materials consists of the linear and isotropic materials, in which:

$$\vec{B} = \mu \vec{H} + \mu_0 \vec{M}_p = \mu \vec{H} + \vec{I}_p \quad (5)$$

where \vec{M}_p is called the permanent magnetization and \vec{I}_p is the magnetic polarization. This category includes the materials for which the temporary magnetization law is (Răduleț, 1975):

$$\vec{M}_t = \chi_m \vec{H} \quad (6)$$

where χ_m is called the magnetic susceptibility, representing a dimensionless and constant scalar quantity.

In the absence of permanent magnetization ($\vec{M}_p = 0, \vec{I}_p = 0$) the relation becomes:

$$\vec{B} = \mu \vec{H} \quad (7)$$

$$\vec{H} = \nu \vec{B}. \quad (8)$$

The quantity μ is the magnetic permeability and $\nu = \frac{1}{\mu}$ is called the reluctivity. The \vec{B} and \vec{H} vectors are collinear.

2.2.2. Linear and non-isotropic materials

In these materials, the \vec{B} and \vec{H} vectors are not, generally, collinear, but the connection between them remains linear.

For some crystalline materials, the dependence between \vec{M}_t and \vec{H} is linear, but each component of the temporary magnetization depends on all components of the magnetic field.

The relation between them can be written, in the absence of permanent magnetization, under the form:

$$\vec{B} = \overset{=}{\mu} \vec{H} \quad (9)$$

where $\overset{=}{\mu}$ is a tensor. In Cartesian coordinates, the relation becomes:

$$\begin{bmatrix} B_x \\ B_y \\ B_z \end{bmatrix} = \begin{bmatrix} \mu_{xx} & \mu_{xy} & \mu_{xz} \\ \mu_{yx} & \mu_{yy} & \mu_{yz} \\ \mu_{zx} & \mu_{zy} & \mu_{zz} \end{bmatrix} \cdot \begin{bmatrix} H_x \\ H_y \\ H_z \end{bmatrix} \quad (10)$$

The permittivity matrix is symmetrical ($\mu_{ij} = \mu_{ji}$) and positively defined. In these conditions, there are three orthogonal directions, called main directions, with respect to which the relation between \vec{B} and \vec{H} becomes (Hănișă, 2004):

$$\begin{bmatrix} B_1 \\ B_2 \\ B_3 \end{bmatrix} = \begin{bmatrix} \mu_1 & 0 & 0 \\ 0 & \mu_2 & 0 \\ 0 & 0 & \mu_3 \end{bmatrix} \cdot \begin{bmatrix} H_1 \\ H_2 \\ H_3 \end{bmatrix} \quad (11)$$

2.2.3. Non-linear and isotropic materials, without permanent magnetization

In these materials, the \vec{B} and \vec{H} vectors are collinear, but the relation between them is non-linear:

$$B = f(H) \quad f: \mathbb{R}^3 \rightarrow \mathbb{R}^3. \quad (12)$$

This is, usually, the behavior of ferromagnetic materials, which are frequently used in the production of electric equipment.

2.2.4. Hysteresis materials

In hysteresis materials, the instantaneous value of the magnetic induction depends not only on the value of the intensity of the magnetic field, but also on the previous evolution of these quantities.

Assume that the magnetic field intensity is gradually reduced after following the first magnetization curve OA , corresponding to a value $+H_{max}$ (Figure 1).

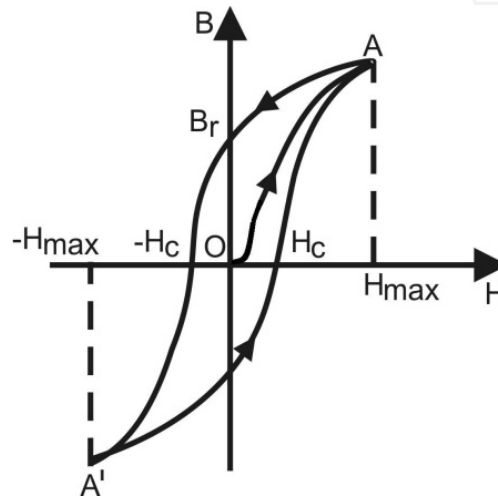


Figure 1. The B - H relation for a hysteresis material

The curve obtained during the magnetic field intensity reduction differs from the first magnetization curve. When H is null, the magnetic induction has a value different from zero called the residual magnetic induction:

$$B_r = \mu_0 \cdot M_r \quad (13)$$

where M_r is the residual magnetization.

For further reduction of the magnetic induction, the sense of magnetic field intensity is changed (as well as the sense of magnetization current), with respect to the initial one.

The magnetic field intensity necessary to compensate the magnetic induction is called the coercive field H_c . Increasing the field in the contrary sense to $-H_{max}$ and then returning to the values of H up to H_{max} , the hysteresis cycle is obtained. By repeating several times the magnetization cycle between the limits $+H_{max}$ and $-H_{max}$, a closed curve and a stabilized cycle are obtained, with the reversal points A and A' symmetrical with respect to the origin of the coordinate system.

It is important to mention that in the case of a periodic magnetization, the existence of the hysteresis cycle leads to energy losses that occur in the ferromagnetic core as heat. These energy losses are called the hysteresis iron losses (Şora, 1982).

2.2.5. Non-linear and non-isotropic materials

In these materials, the \vec{B} and \vec{H} vectors are not, generally, collinear and the relation between them is non-linear.

2.3. The magnetic vector potential

The magnetic vector potential is a vector field, which does not have a specific physical meaning. Its utilization allows simplification of the mathematical approach of many physical problems.

The condition $div \vec{B} = 0$, which expresses the continuity of the magnetic flux, is identically satisfied if the \vec{B} vector is expressed under the form of an auxiliary vector \vec{A} , called the magnetic potential vector:

$$\vec{B} = rot \vec{A} \quad (14)$$

The potential vector \vec{A} is univocally determined only after $div \vec{A} = 0$ is chosen. The choice of the value for \vec{B} is called the calibration of the vector potential and the respective condition is called calibration condition. Depending on the context, one can adopt convenient *calibration conditions*. One of the most used calibration conditions is the Coulomb condition:

$$div \vec{A} = 0 \quad (15)$$

If the calculation of the magnetic flux through an open surface is expressed by means of magnetic induction, then the magnetic vector potential must be taken into account by the Stokes' theorem (Moraru, 2002).

The *magnetic flux* through a surface S_r bounded by a contour Γ can be computed as a contour integral of the vector potential:

$$\Phi_{S_r} = \int_{S_r} \vec{B} d\vec{A} = \int_{S_r} rot \vec{A} d\vec{A} = \oint_{\Gamma} \vec{A} d\vec{l} \quad (16)$$

The magnetic flux through the surface S_r is equal to the line integral of the magnetic vector potential along the contour Γ on which this surface is supported. Equation (16) relieves the fact that the value of a magnetic flux does not depend on the surface shape, as it is computed only by considering the contour on which that surface is supported. Let us consider a material with linear magnetic properties and without permanent magnetization, for which $\vec{B} = \mu \vec{H}$. From the magnetic circuit law, it results that (Hăntîlă, 2004):

$$rot \vec{H} = rot \left[\frac{1}{\mu} rot \vec{A} \right] = \vec{j} \quad (17)$$

In linear and homogeneous mediums, where μ is constant:

$$\text{rot rot } \vec{A} = \mu \vec{J} = \text{grad div } \vec{A} - \Delta \vec{A} \quad (18)$$

the magnetic vector potential verifies the *Poisson's* vector equation:

$$\Delta \vec{A} = -\mu \vec{J} \quad (19)$$

and if $\vec{J} = 0$, it verifies the *Laplace's* equation:

$$\Delta \vec{A} = 0 \quad (20)$$

Solving Equations (19) and (20) requires the boundary condition to be known. The vector equations are divided after the Cartesian coordinates in scalar equations of Poisson type

$$\Delta A_x = -\mu J_x \quad \Delta A_y = -\mu J_y \quad \Delta A_z = -\mu J_z \quad (21)$$

respectively, scalar equations of Laplace type

$$\Delta A_x = 0 \quad \Delta A_y = 0 \quad \Delta A_z = 0. \quad (22)$$

The integral of Equation (19) in all space is determined by using the scalar forms (21).

The magnetic vector potential of the filiform circuit with current i is expressed as:

$$\vec{A} = \frac{\mu \cdot i}{4\pi} \oint_{\Gamma} \frac{d\vec{l}}{R}, \quad (23)$$

$d\vec{l}$ is line unit vector.

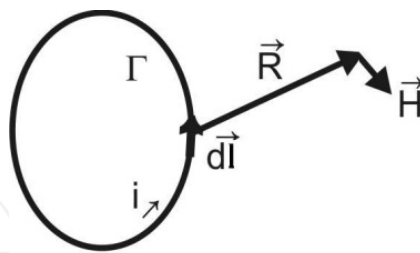


Figure 2. Biot-Savart-Laplace relation for filiform conductors

The magnetic field intensity is (Figure 2):

$$\vec{H} = \frac{\text{rot } \vec{A}}{\mu} = \frac{i}{4\pi} \oint_{\Gamma} \frac{d\vec{l} \times \vec{R}}{R^3}. \quad (24)$$

The Biot-Savart-Laplace relation becomes:

$$\vec{B} = \frac{\mu}{4\pi} \int_{D_{\infty}} \frac{\vec{J} \times \vec{R}}{R^3} \quad (25)$$

2.4. The scalar magnetic potential

The magnetic field is not irrotational for a circuit with current flow, therefore this can be deduced from a scalar potential. But the rotor of magnetic field intensity is equal to zero if there is no current which flows, $\vec{J} = 0$. If there is no conductor in the considered space, the following equation is available (Mocanu, 1981):

$$\text{rot } \vec{H} = 0 \tag{26}$$

Therefore, \vec{H} can be deduced by a scalar potential:

$$\vec{H} = -\text{grad} V_m \tag{27}$$

where is V_m is the scalar magnetic potential.

In the presence of some conductors crossed by electric current, the scalar magnetic potential is not uniform:

$$\int_1^2 \vec{H} d\vec{l} = i = -\int_1^2 \nabla V_m dl = -\int_1^2 dV = V_{m1} - V_{m2} \neq 0 \tag{28}$$

For uniformity, a cut can be introduced an arbitrary surface bounded by the contour crossed by current (Figure 3).

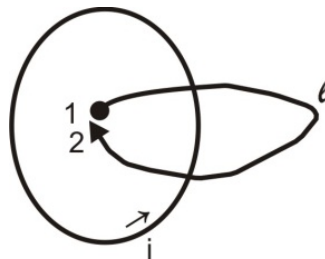


Figure 3. Cut in order to uniform the scalar magnetic potential

In the absence of permanently magnetized bodies, the partial derivative equation of the scalar magnetic potential is deduced from the magnetic flux law:

$$\vec{B} = -\mu \nabla V_m \quad \text{div } \vec{B} = 0 \rightarrow -\text{div}(\mu \nabla V_m) = 0 \tag{29}$$

In homogeneous materials (where $\mu = \text{const}$), the Laplace equation is obtained:

$$\nabla V_m = 0 \tag{30}$$

This expression is used to determine the scalar magnetic potential of the magnetic field produced by a filiform circuit crossed by electric current.

Applying the magnetic circuit law for a closed curve which surrounds the conductor, the scalar magnetic potential is written as:

$$V_m = \frac{i}{4\pi} \Omega \quad (31)$$

where Ω is the solid angle under which the Γ contour is seen from the point where the field is calculated:

$$\Omega = \int_{S_r} \frac{R}{R^3} dS \quad (32)$$

In this case, the magnetic field intensity \vec{H} is:

$$\vec{H} = -\frac{1}{4\pi} i \nabla \Omega \quad (33)$$

2.5. Energy of the stationary magnetic field

Magnetic energy is located in a magnetic field with a volume density w_m whose expression is (Şora, 1982):

$$w_m = \int_0^B \vec{H} d\vec{B} \quad (34)$$

If the medium is linear ($\mu = \text{constant}$), then:

$$H dB = H d(\mu H) = d\left(\frac{\mu H^2}{2}\right) \quad (35)$$

In this case, the following expressions are obtained:

$$w_m = \frac{\mu H^2}{2} = \frac{B^2}{2\mu} = \frac{\vec{H} \vec{B}}{2} \quad (36)$$

$$W_m = \frac{1}{2} \int_v \vec{H} \vec{B} dv \quad (37)$$

Assuming that inside the field limited by a closed surface Σ and considering an isotropic medium, the magnetic energy can be written as:

$$\text{div}(\vec{A} \cdot \vec{H}) = \vec{H} \text{rot} \vec{A} - \vec{A} \text{rot} \vec{H} \quad (38)$$

taking into account the vector operation.

In other words, the magnetic energy is:

$$W_m = \frac{1}{2} \int_v \vec{H} \text{rot} \vec{A} dv = \frac{1}{2} \int_v \text{div}(\vec{A} \cdot \vec{H}) dv + \frac{1}{2} \int_v \vec{A} \vec{J} dv \quad (39)$$

Applying the Gauss-Ostrogradski's theorem to the first term on the right-hand side, the following expression is obtained:

$$W_m = \frac{1}{2} \int_{\Sigma} (\vec{A} \cdot \vec{H}) d\vec{s} + \frac{1}{2} \int_v \vec{A} \vec{J} dv \quad (40)$$

2.6. Generalized forces in the stationary magnetic field

In the case of the stationary magnetic field, the general expressions of the generalized forces X_k associated to a generalized coordinate x_k are given by one of the two generalized forces theorems in a stationary magnetic field (Timotin, 1970):

$$X_k = - \left[\frac{\partial W_{em}}{\partial x_k} \right]_{\Phi=ct} \quad (41)$$

$$X_k = \left[\frac{\partial W_{em}}{\partial x_k} \right]_{i=ct} \quad (42)$$

in which the transformations are supposed to be done at constant fluxes on any surface, respectively to constant currents through any conducting contour.

2.7. Uniqueness theorems of the solutions of the equations of stationary and magnetostatic magnetic fields

2.7.1. The enunciation of stationary and magnetostatic magnetic field

In stationary magnetic field problems, the electric currents distribution (the \vec{J} field) is supposed to be known (for example, by solving a stationary electrokinetic stationary regime, in the case of massive conductors, or by indicating the value of the current through the coils in the domain that is being studied).

In magnetostatic field problems, the sources of the field are represented by the distribution of the permanent magnetization (\vec{M}_p or the permanent magnetic polarization), which are supposed to be known (Andrei et al, 2012).

In conformity to the general uniqueness theorem of the solutions of the stationary magnetic fields equations, the solution of the electromagnetic field equations in a domain D_{Σ} bounded by closed surface $\Sigma = S_H \cup S_B$ is uniquely determined by the following uniqueness conditions:

The electric currents distribution in the domain:

$$J(P); \quad \forall P \in D_{\Sigma} \quad (43)$$

The distribution of the permanent magnetization:

$$M_p(P); \quad \forall P \in D_{\Sigma} \quad (44)$$

Boundary conditions, that can be of the following types (Figure 4):

- tangent component of the magnetic field intensity on the surface S_H :

$$H_t(P) = f(p); \quad \forall P \in S_\Sigma \quad (45)$$

- normal component of the magnetic induction on the surface S_B :

$$B_n(P) = g(p); \quad \forall P \in S_\Sigma \quad (46)$$

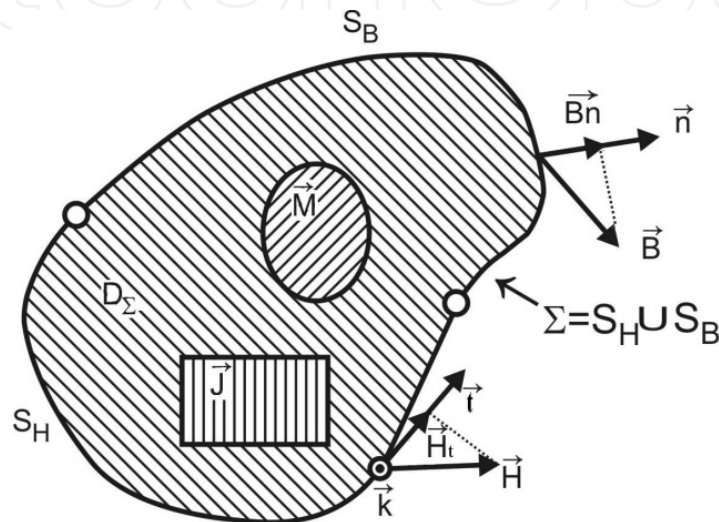


Figure 4. The uniqueness theorem for the stationary magnetic field (Andrei et al. 2012)

The theorem stands for linear materials, or for non-linear materials, but having B - H monotone magnetization characteristics. The case of materials which have hysteresis is not included. Particular forms can be deduced from this general formulation, expressed by field potentials.

2.7.2. The enouncing by scalar magnetic potential (magnetostatic field problems)

In magnetostatic regime problems, the sources of the magnetic field are represented by the permanent magnetization of the bodies (Andrei et al., 2012).

The boundary conditions, expressed by the scalar magnetic potential, are of the following types:

- Dirichlet Conditions, which consist of imposing values for the scalar magnetic potential at the points on the surface, denoted by S_D :

$$V(P) = f(P); \quad \forall P \in S_D \quad (47)$$

These conditions imply knowing the value of the tangent component of the intensity of the magnetic field in the respective points, which is equal to the derivative by the tangent direction of the scalar magnetic potential (Fluerașu & Fluerașu, 2007).

- b. Neumann Conditions, which consist of imposing the values of the derivative of the scalar magnetic potential in the direction of the normal to the surface, denoted by S_N . Practically, this type of conditions imposes the normal component of the magnetic induction in the respective points on the surface:

$$B_n = -\mu \frac{dV}{dn} = g(P); \quad \forall P \subset S_N \quad (48)$$

- c. mixed conditions, that consist of imposing a condition in the form of a linear combination between the two above condition types, on a portion S_M of the surface.

$$\alpha V + \beta \frac{dV}{dn} = h(P); \quad \forall P \subset S_M \quad (49)$$

3. Finite element analysis

3.1. Triangular finite elements

The first step in solving the problems using the Finite Element Method (FEM) begins by dividing the analysis area in finite elements, as well as the choice of the finite element type. Currently, a wide range of finite elements is used, but their classification, their description, as well as their criteria presentation for choosing adequate finite element types does not represent the subject of this chapter. In the presented application, the triangular finite element with three nodes is used. At the same time with the choice of finite element type, the shape functions are chosen, so that the description of finite elements is followed by the associated shape function presentation. Concerning the shape functions, the interpolating polynomials are mainly used due to the facility in their derivation and their integration. The interpolation on a triangle supposes a shape or interpolating function which links the nodal values (triangle vertices). An approximation of the solution of the magnetic vector potential \vec{A} is allowed at the level of each triangular element „e” (Figure 5), according to the following interpolating polynomial (Stammberg, 1995):

$$\alpha_k = a_k + b_k \cdot x + c_k \cdot y \quad (50)$$

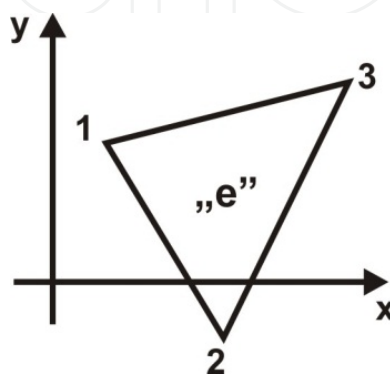


Figure 5. The triangular element „e”

The shape function coefficients a_k , b_k , and c_k are called the generalized coordinates. These coefficients are constant because they depend on the constant coordinates of the nodes only.

The values of the shape functions vary between 0 and 1. They are equal to 1 in node k and linearly decrease in the elements adjacent to this node, being null in the rest of the nodes and elements (Figure 6). Thus:

$$\begin{aligned} \alpha_k(x = x_k, y = y_k) &= 1 & k = 1, 2, 3 \\ \alpha_k(x = x_i, y = y_i) &= 0 & i \neq k \end{aligned} \quad (51)$$

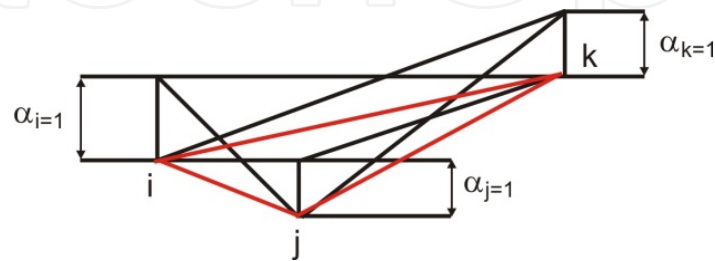


Figure 6. Graphical representation of the shape function

The shape function α_1 for node 1 results from the formula (Stammberg, 1995):

$$\begin{pmatrix} 1 & x_1 & y_1 \\ 1 & x_2 & y_2 \\ 1 & x_3 & y_3 \end{pmatrix} \cdot \begin{pmatrix} a_1 \\ b_1 \\ c_1 \end{pmatrix} = \begin{pmatrix} 1 \\ 0 \\ 0 \end{pmatrix}. \quad (52)$$

The shape function coefficients are:

$$\begin{aligned} a_k &= \frac{x_{i+1} \cdot y_{i+2} - x_{i+2} \cdot y_{i+1}}{D} \\ b_k &= \frac{y_{i+1} - y_{i+2}}{D} \\ c_k &= \frac{x_{i+2} - x_{i+1}}{D} \end{aligned} \quad (53)$$

where:

$$D = x_2 y_3 - x_3 y_2 - x_1 y_3 + x_1 y_2 + x_3 y_1 - x_2 y_1 \quad (54)$$

and the index i takes the values by circular permutations in nodal set of an element „ e “, in clockwise order. Writing with S_e , the area of element „ e “:

$$S_e = \frac{1}{2} \begin{vmatrix} 1 & x_1 & y_1 \\ 1 & x_2 & y_2 \\ 1 & x_3 & y_3 \end{vmatrix} \quad (55)$$

Considering:

$$D = 2S_e \quad (56)$$

The magnetic vector potential in an arbitrary point (x,y,z) is obtained with the following equation:

$$A(x,y,z) = \sum_{k=1}^{n(e)} \alpha_k(x,y,z) A_k \quad (57)$$

where:

α_k - shape function

$n(e)$ - number of nodes on element

A_k - magnetic vector potential of node k

3.2. FEM application for two-dimensional problems of stationary magnetic field

Finite element methods (FEM) use most of the times a variation principle. According to the variation computation, solving a differential equation in a field and under certain boundary conditions is equivalent with minimizing, in that field, a functional corresponding to the differential equation with its boundary conditions. A functional integral is an integral expression, a function that depends on the unknown functions. The functional integral has a finite value.

The problem concerning solving the system of differential equations of the electromagnetic field with some boundary conditions is equivalent with the problem of finding a function which gives the integral minimum by which the energy system is expressed.

Let's consider the energy functional associated with the arbitrary three-dimensional field D :

$$\mathfrak{S} = \int_{\mathcal{D}} \left\{ \left(\int_0^{\vec{E}} \vec{D} d\vec{E} - \int_0^{\vec{B}} \vec{H} d\vec{B} \right) + (\vec{J}\vec{A} - \rho_V V) \right\} d\mathcal{D} \quad (58)$$

where $\vec{D}, \vec{E}, \vec{B}, \vec{H}$ are the vectors associated with electric and magnetic fields, \vec{A} is the magnetic vector potential, V is the scalar electric potential, \vec{J} is the density vector of conduction electric current and is the volume density of electric charge (Silvester & Ferrari, 1996).

The first parenthesis of the integrand represents the difference between the volume density of the electric and magnetic energy. The second parenthesis represents the difference between the volume density of interaction energies between the conduction current and magnetic field, as well as between the electric charge and the electric field. The interaction energies are equal to the work done by the field forces in order to bring the current density, respectively electric charge, from infinity, where the potentials are considered $(\vec{A} = 0, V = 0)$, to the states characterized by the values \vec{A} and V .

The electromagnetic potentials \vec{A} and V define the vectors \vec{E} and \vec{B} of the electromagnetic field:

$$\vec{E} = -\text{grad } V \quad (59)$$

and

$$\vec{B} = \text{rot } \vec{A} \quad (60)$$

The energy functional associated with the stationary magnetic field produced by the direct currents and in case by permanent magnets is expressed as:

$$\mathfrak{S}(\vec{A}) = \int_{\mathcal{D}} \left(\int_0^{\vec{B}} \vec{H} d\vec{B} - \vec{j} \vec{A} \right) d\mathcal{D} \quad (61)$$

Two-dimensional problems of stationary magnetic field are by definition problems in which the unknown, the vector magnetic potential \vec{A} , is orientated as one axis of the coordinate system and depends on the other two coordinates of the system (Stammberg, 1995).

2D problems in Cartesian coordinates (x,y,z) are called parallel-plane. The current density \vec{j} is oriented by the axis Oz and the magnetic vector potential has the structure $\vec{A} = A\vec{k}$ and its orientation is also by the axis Oz. The magnetic induction is written as:

$$\vec{B} = \text{rot} \vec{A} = \begin{vmatrix} \vec{i} & \vec{j} & \vec{k} \\ \frac{\partial}{\partial x} & \frac{\partial}{\partial y} & \frac{\partial}{\partial z} \\ 0 & 0 & A(x,y) \end{vmatrix} = \vec{i} \frac{\partial A}{\partial y} - \vec{j} \frac{\partial A}{\partial x} = \vec{k} \times (-\text{grad} A) \quad (62)$$

The square of magnetic induction is:

$$\vec{B}^2 = (\text{rot } \vec{A})^2 = \begin{pmatrix} \frac{\partial A}{\partial y} \\ -\frac{\partial A}{\partial x} \\ 0 \end{pmatrix}^2 = \left(\frac{\partial A}{\partial y} \right)^2 + \left(\frac{\partial A}{\partial x} \right)^2 = (\text{grad } A)^2. \quad (63)$$

The magnetic vector potential \vec{A} is obtained by minimizing the functional:

$$\delta \mathfrak{S}(\vec{A}) = 0 \quad (64)$$

In the case of stationary magnetic field, the functional is related to the physical size of a known issue, such as the total energy of the magnetic field inside the domain D :

$$W_m = \frac{1}{2} \int_V \vec{H} \cdot \vec{B} dv \quad (65)$$

The magnetic energy is located in the magnetic field with the volume density w_m :

$$w_m = \frac{\vec{H} \cdot \vec{B}}{2} = \frac{\vec{B}^2}{2\mu} \tag{66}$$

Eckhardt describes in detail the solution to this problem. The magnetic field density is reduced to the following scalar equation (Stammberg, 1995; Eckhardt, 1978):

$$w_m = \frac{1}{2\mu} B^2 - J \cdot A = \frac{1}{2\mu} \left[\left(\frac{\partial A}{\partial x} \right)^2 + \left(\frac{\partial A}{\partial y} \right)^2 \right] - J \cdot A \tag{67}$$

In the case of the parallel-plane fileds, the boundary conditions are:

$$A(x, y) = f(P), \quad P \in C_D \tag{68}$$

$$-\frac{1}{\mu} \frac{dA}{dn} \Big|_{C_N} = g(P), \quad P \in C_N \tag{69}$$

where Eq. (68) represents the Dirichlet boundary conditions on the boundary C_D and Eq. (69) represents the Neumann boundary conditions on the boundary C_N . The unknown function $A(x, y)$ is the solution of the Poisson’s equation in a two-dimensional domain, the boundary Γ being composed of two disjoint parts C_D and C_N where the Neumann and Dirichlet conditions are described (Figure 7):

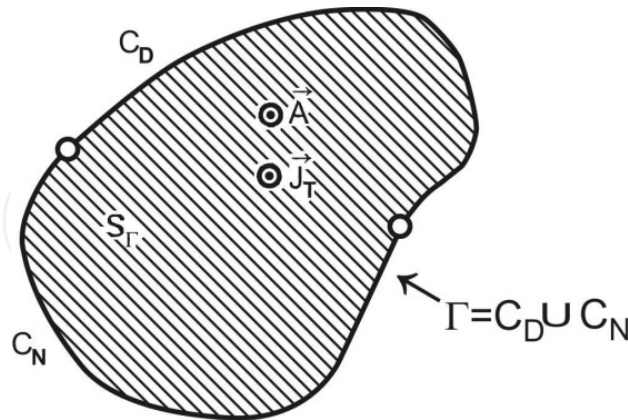


Figure 7. The domain of computation for a two-dimensional problem (Andrei et al. 2012)

$$\ell = \int_S \left\{ \frac{1}{2\mu} \left[\left(\frac{\partial A}{\partial x} \right)^2 + \left(\frac{\partial A}{\partial y} \right)^2 \right] - J \cdot A \right\} dx dy \tag{70}$$

where the function ℓ represents the magnetic energy computed on the surface S_r bounded by the curve Γ . The unknown function $A(x, y)$ for node i is determined by minimizing the functional:

$$\frac{\partial \ell}{\partial A_i} = \int_S \left\{ \frac{1}{\mu} \left[\frac{\partial A}{\partial x} \cdot \frac{\partial}{\partial A_i} \left(\frac{\partial A}{\partial x} \right) + \frac{\partial A}{\partial y} \cdot \frac{\partial}{\partial A_i} \left(\frac{\partial A}{\partial y} \right) \right]^2 - J \frac{\partial A}{\partial A_i} \right\} dx dy = 0 \quad (71)$$

Therefore, the following equations system is obtained:

$$f_k = \sum_{z=1}^{q(i)} \frac{\partial \ell}{\partial A_i} = 0 \quad (72)$$

A_i is the magnetic vector potential of the node i of the element z .

The differentials involved in Eq. (71) are written according to the shape functions and have the following expressions (Stammberg, 1995; Eckhardt, 1978):

$$\frac{\partial A}{\partial x} = \sum_{k=1}^{n(e)} A_k \frac{\partial \alpha_k}{\partial x} = \sum_{k=1}^{n(e)} A_k \cdot b_k \quad (73)$$

$$\frac{\partial A}{\partial y} = \sum_{k=1}^{n(e)} A_k \frac{\partial \alpha_k}{\partial y} = \sum_{k=1}^{n(e)} A_k \cdot c_k \quad (74)$$

$$\frac{\partial}{\partial A_i} \left(\frac{\partial A}{\partial x} \right) = \frac{\partial \alpha_i}{\partial x} = b_i \quad (75)$$

$$\frac{\partial}{\partial A_i} \left(\frac{\partial A}{\partial y} \right) = \frac{\partial \alpha_i}{\partial y} = c_i \quad (76)$$

$$\frac{\partial A}{\partial A_i} = \frac{\partial}{\partial A_i} \left(\sum_{k=1}^{n(e)} \alpha_k A_k \right) = \alpha_i = a_i + b_i \cdot x + c_i \cdot y \quad (77)$$

$$\frac{\partial \ell_e}{\partial A_i} = \int_S \left\{ \frac{1}{\mu} \left[\left(\sum_{k=1}^{n(e)} b_k \cdot A_k \right) \cdot b_i + \left(\sum_{k=1}^{n(e)} c_k \cdot A_k \right) \cdot c_i \right] - J \alpha_i \right\} dx dy = 0 \quad (78)$$

A homogeneous medium is considered, thus the magnetic permittivity μ is constant for each finite element, being independent of the x and y coordinates:

$$\frac{\partial \ell_e}{\partial A_i} = \frac{D}{2\mu} \left[A_1 (b_1 b_i + c_1 c_i) + A_2 (b_2 b_i + c_2 c_i) + A_3 (b_3 b_i + c_3 c_i) \right] - J \frac{D}{6} = 0 \quad (79)$$

where D is the determinant computed according to Eq.(56).

Eq. (79) can be written under matrix form as:

$$\frac{\partial \ell_e}{\partial A_i} = \frac{D}{2\mu} (b_1 b_i + c_1 c_i \quad b_2 b_i + c_2 c_i \quad b_3 b_i + c_3 c_i) \cdot \begin{pmatrix} A_1 \\ A_2 \\ A_3 \end{pmatrix} - J \frac{D}{6} = 0 \quad (80)$$

The functional is sum of contributions other than the „*ne*” finite elements. Stationarization of the functional requires (Stammberg, 1995; Silvester & Ferrari, 1996):

$$\sum_{e=1}^{ne} \frac{\partial \ell_e}{\partial A_i} = 0 \quad (81)$$

where „*ne*” is the total number of finite elements.

$$\{F\} = [K] \cdot \{A\} - [P] + [Q] \quad (82)$$

The term $[P]$ is used for the case of the „source” type elements where the current density \bar{J} is non-null, and the term $[Q]$ is used for the case of the elements which have in one of the sizes a non-homogeneous Neumann boundary. By assembling the „*ne*” equations in Eq. (81), a linear system of equations of magnetic vector potential values in the mesh nodes is obtained (Ioan, 1993).

4. Applications

Direct current (DC), which was one of the main means of distributing electric power, is still widespread today in the electrical plants supplying particular industrial applications. The advantages in terms of settings, offered by the applicants of DC motors and by supply through a single line, make direct current supply a good solution for railway and underground systems, trams, lifts and other transport means. Current-limiting circuit breakers play an important role in electrical low-voltage circuits. Due to the high short-circuit currents it is necessary a very short time to switch off the faulted branch. For this reason the current limiting circuit breakers are conceived as elaborated solutions especially for the arc quenching system, meaning the path of current and the arcing chamber (Vîrjoghe, 2010).

This section presents the calculation of the magnetic field in the arcing chamber of a current-limiting d.c. circuit breaker of 1250 A, 750 V, and in a DC circuit breaker-separator of 3150 A, 1000 V. The authors present few optimization solutions of some quenching systems which will lead to more performing constructive choices. Two-dimensional (2D) and three-dimensional (3D) problems of stationary magnetic field are addressed.

The finite element software package ANSYS is used for calculation of the magnetic field components. This tool includes three stages: preprocessor, solver and postprocessor. The procedure for carrying out a static magnetic analysis consists of following main steps: create the physics environment, build and mesh the model and assign physics attributes to each region within the model, apply boundary conditions and loads (excitation), obtain the solution, and review the results (ANSYS Documentation).

A typical magnetic field problem is described by defining its geometry, material properties, currents, boundary conditions, and the field system equations. The computer requires the input data and provides the numerical solution of the field equation and the output of desired parameters. If the values are found unsatisfactory, the design is modified and parameters are recalculated. The process is repeated until optimum values for the design parameters are obtained.

In order to define the physics environment for an analysis, it is necessary to enter in the ANSYS preprocessor (PREP7) and to establish a mathematical simulation model of the physical problem. In order to this, the following steps are presented below: set GUI Preferences, define the analysis title, define the element types and options, define the element coordinate systems, set real constants and define a system of units, and define the material properties (ANSYS Documentation).

The Global Cartesian coordinate system is the default. A different coordinate system can be specified by the user by indicating its origin location and orientation angles. The coordinate system types are Cartesian, cylindrical (circular or elliptical), spherical, and toroidal.

Some materials with magnetic properties are defined in the ANSYS material library. The materials can be modified to correspond more closely to the analysed problem and to be loaded in the ANSYS database. The copper property shows temperature which depends on resistivity and relative permeability. All other properties are described in terms of B - H curves. Most of the materials included in ANSYS are used for modeling the electromagnetic phenomenon. The element types are used to establish the physics of the problem domain. Some element types and options are defined to represent the different regions in the model. If some laminated materials are aligned in an arbitrary form, the element coordinate system or systems have to be identified and used. The applications presented in this chapter use the PLANE53 element in the two-dimensional problem and the SOLID97 element for the three-dimensional problem.

In order to obtain the magnetic field values, the Maxwell's equations are solved by using the input data. The nodal values of the magnetic vector potential are considered as main or primary unknowns. Their derivatives (e.g., flux density) are the secondary unknowns. After this, it is possible to choose the type of solver to be used. The available options include Sparse solver (default), Frontal solver, Jacobi Conjugate Gradient (JCG) solver, JCG out-of-memory solver, Incomplete Cholesky Conjugate Gradient (ICCG) solver, Preconditioned Conjugate Gradient solver (PCG), and PCG out-of-memory solver (ANSYS Documentation).

The results of the calculations are shown in the postprocessing phase, which is a graphical program. Here, it can be observed if the applied loads affect the design, if the finite element mesh is good, and so on. The resulting fields in the form of contour and density plots are displayed by this graphical program. The analysis of the field at arbitrary points, the evaluation of a number of different integrals, and the plot of some quantities along pre-defined contours are also made with this program. The plotted results are saved in the Extended Metafile (EMF) format.

4.1. Numerical modelling of stationary magnetic field in area slope-slider-ferromagnetic profile of arc chamber in case of a current-limiting DC circuit breaker – 2D application

The problem of magnetic field distribution in the arc chamber of DC a circuit breaker with rated current 1250A was numerically solved. The conductor where a current of 1250 A flows is located in the immediate vicinity of a ferromagnetic profile. This has the role of enhancing and orienting the magnetic field in the arc-quenching chamber for obtaining a strong force that moves the arc up inside the extinction chamber (Vîrjoghe, 2004).

It is considered the plane parallel model, whose cross section is shown in Figure 8. This model is an I shaped ferromagnetic profile, with cross section in the vertical plane and the dimensions of 60x3 mm². The cross section of copper conductor is 5x15 mm². The conductor is surrounded by a slider with U shaped cross section and a thickness of 1mm.

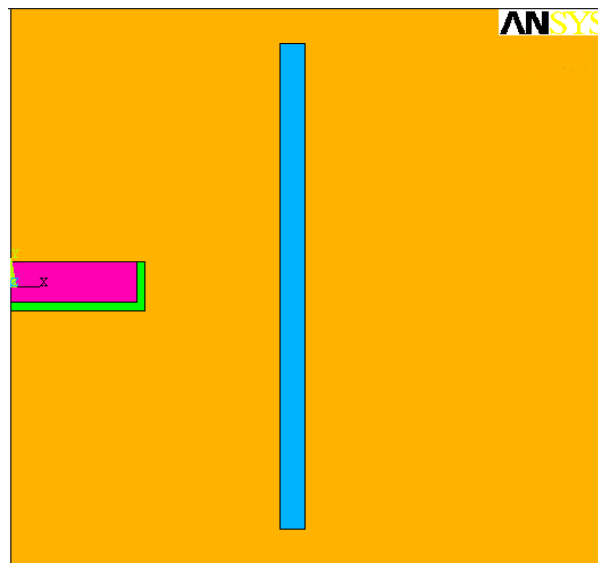


Figure 8. The physical model in the area with ramp, slider and ferromagnetic profile

For numerical computation the *PLANE53* element was chosen, which allows two-dimensional modeling of the magnetic field in plane parallel and axisymmetric problems. This element is based on the magnetic vector potential formulation with Coulomb calibration. This element is also applicable to the stationary magnetic field with the possibility of modeling the magnetic nonlinearities. The material used for other two ferromagnetic profiles is a steel chosen from the ANSYS library and having the properties in the *emagM3.SI_MPL* folder. The material is M3 steel and its magnetization curve is shown in Figure 9. This domain was discretized in a number of 2436 triangular finite elements uniformly distributed (Vîrjoghe, 2004).

The boundary conditions and loads are applied to a 2-D static magnetic analysis either on the solid model (key points, lines, and areas) or on the finite element model (nodes and elements). The loads applied to the solid model to the mesh during solution are automatically transferred by ANSYS (ANSYS Documentation).

To observe the influence of the ferromagnetic slider and of the ferromagnetic plate on the magnetic field distribution, the magnetic induction is computed and the magnetic flux lines are drawn. The slider and the ferromagnetic plate case were studied independently of each other.

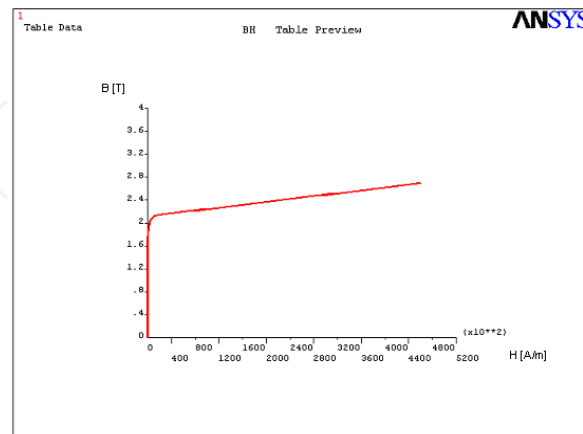


Figure 9. The magnetization characteristic for the M3 steel

Figure 10 and Figure 11 respectively show the magnetic induction spectrum and the magnetic field lines only, for the case of ferromagnetic slider.

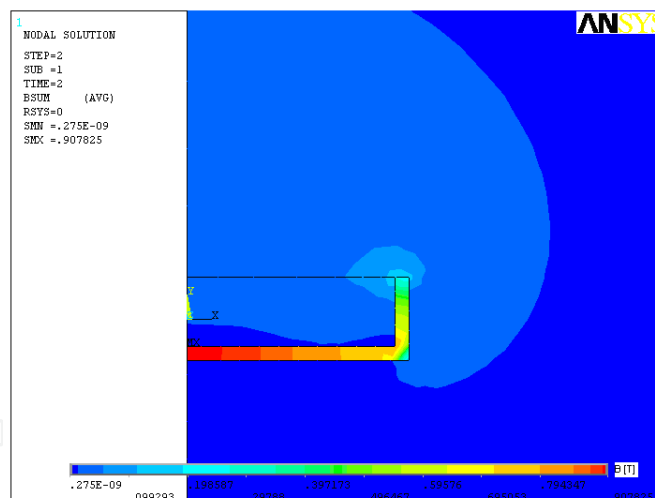


Figure 10. The magnetic induction spectrum in the presence of the ferromagnetic slider

Figure 12 and Figure 13 respectively show the magnetic induction spectrum and the magnetic field lines only, for the case of *I* shaped ferromagnetic profile. Figure 14 and Figure 15 respectively show the magnetic induction spectrum and the magnetic field lines when using the ferromagnetic profile and the ferromagnetic slider (Vîrjoghe, 2004).

Analyzing these simulations, a strong influence of the ferromagnetic slider on the orientation of the magnetic field was observed. When using only the ferromagnetic slider, a shielding of the field lines is observed, and the maximum values of the magnetic induction is 0.907 T. The *I* shaped ferromagnetic profile makes a good shielding of the field lines

obtaining the maximum values of magnetic induction of 0.153 T. If both methods of magnetic field orientation are used together then a maximum value of magnetic induction of 0.947 T is obtained. To obtain the system optimization in this area, the simulations for a thickness of 2 mm have been repeated.

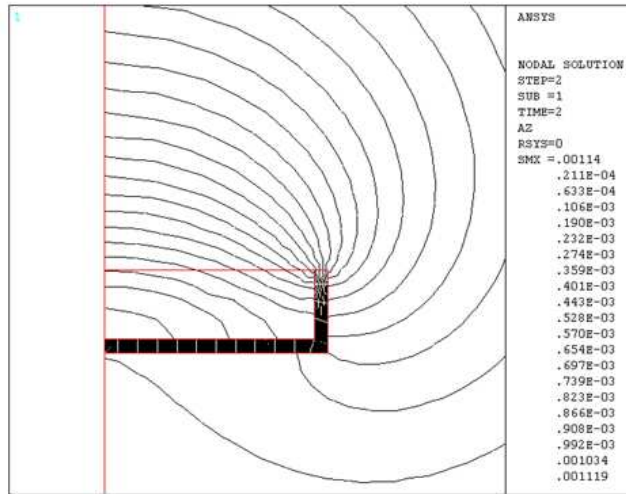


Figure 11. The magnetic equipotential lines in the presence of the ferromagnetic slider

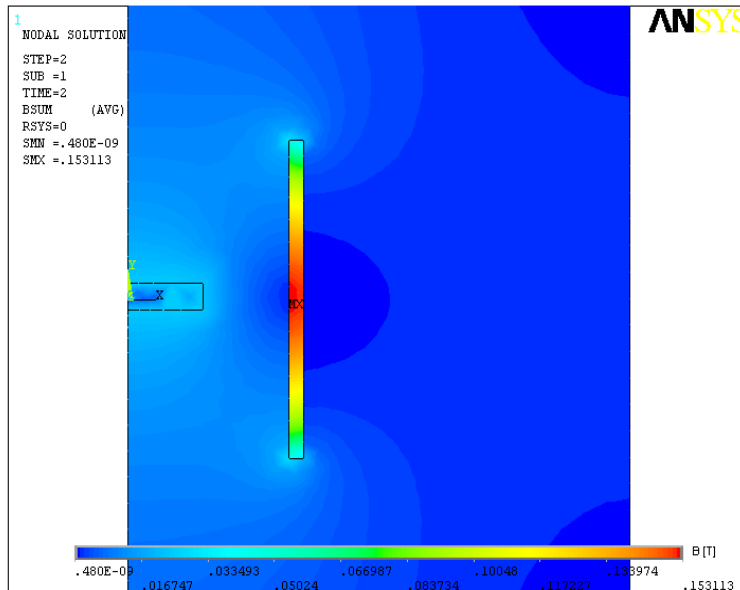


Figure 12. The magnetic induction spectrum in the case with the ferromagnetic profile

Thus, the obtained results are plotted in comparison with those presented for the slider of 1 mm (Figure 16). For the slider with the thickness of 2 mm, the values of magnetic induction are lower (up to 0.5 T). Using the slider of 1 mm thickness a better orientation of the field lines, as well as a better arc transmission toward arc-quenching chamber are observed. The path for the displayed charts is chosen between two points placed symmetrically one from another in the middle of a figure which contains the conductor, slider and ferromagnetic profile (Vîrjoghe, 2004).

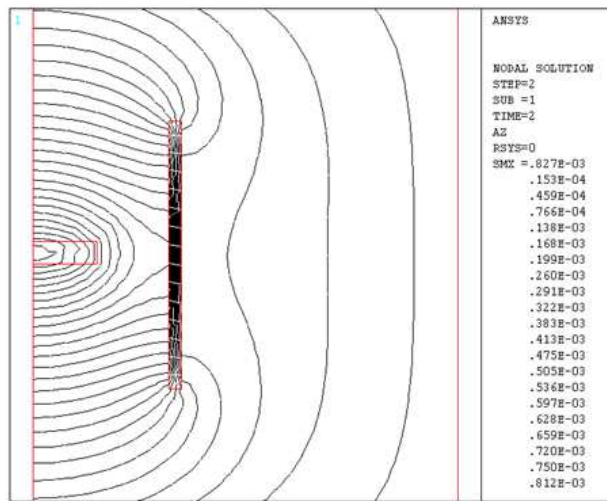


Figure 13. The magnetic equipotential lines in the presence of the ferromagnetic profile

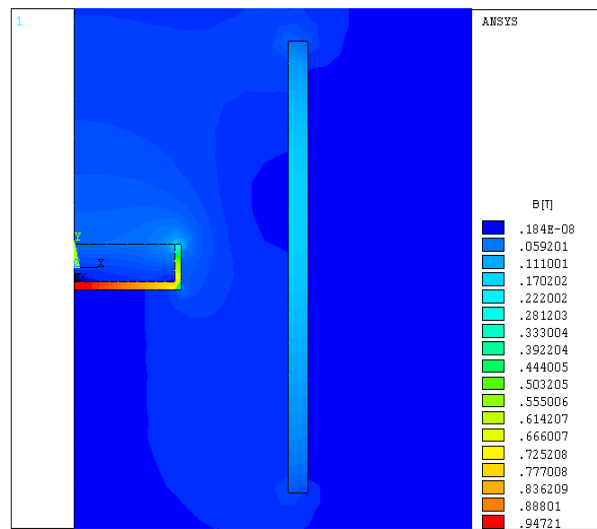


Figure 14. The magnetic induction spectrum in the area with ramp, slider and ferromagnetic profile.

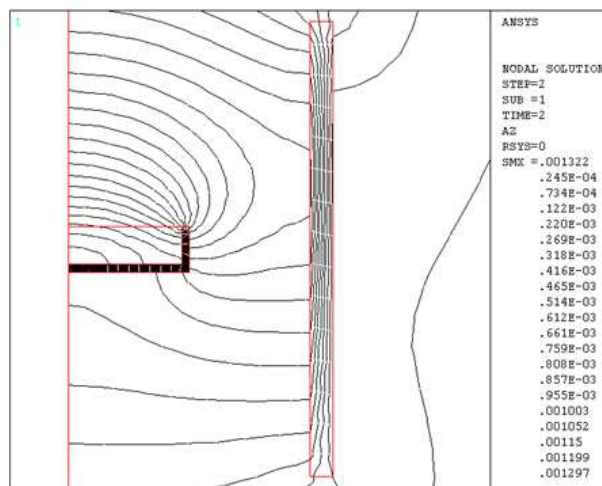


Figure 15. The magnetic equipotential lines in the area with ramp, slider and ferromagnetic profile.

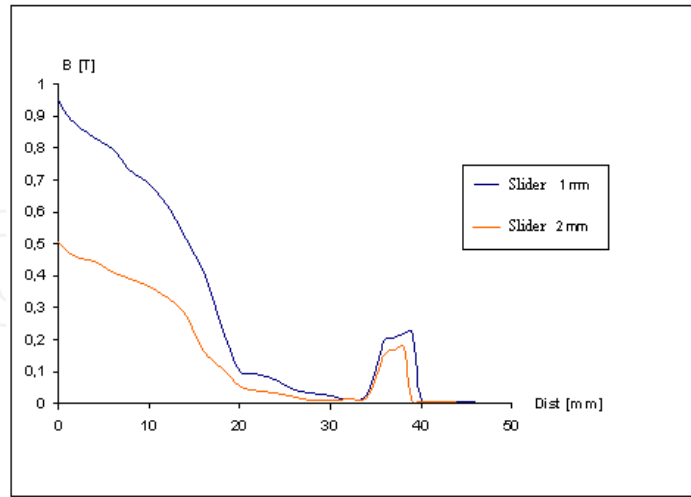


Figure 16. Magnetic induction variation depending on the thickness of the slider.

4.2. Numerical modelling of stationary magnetic field of arc-quenching chamber in case of a DC circuit breaker-separator – 3D application

The physical model of the arc-quenching chamber in case of a DC circuit breaker-separator of 3125 A having the ramps-ferromagnetic profiles is shown in Figure 17. In this model, two profiles composed of a ferromagnetic material are presented. The magnetization curve of the two profiles is shown in Figure 9.

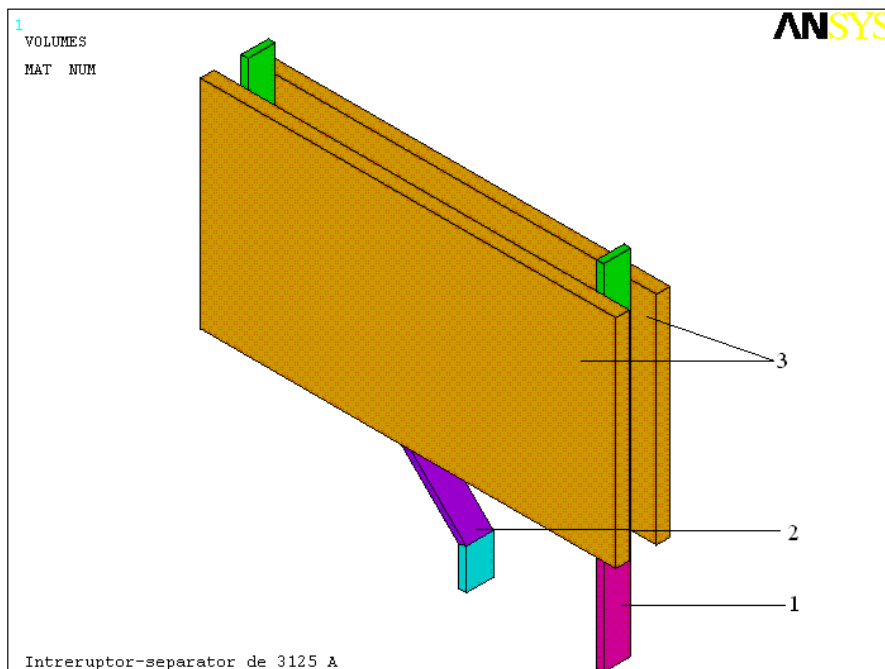


Figure 17. The DC circuit breaker-separator model with a current of 3125A.

These profiles form a rectangular prism with length of 150 mm, height of 100 mm and thickness of 5 mm. The electric arc ramps 1 and 2 are made of copper and have width of 10mm and thickness of 2.5 mm. The left ramp is inclined to the vertical with an angle of 45°.

The arc chamber model together with ramps 1 and 2 are incorporated in a boundary volume, where the air is defined as material. In order to achieve the circuit continuity, two ramps have been unified with a bar 3 having the same dimensions of the ramps (Figure 18).

In the preprocessing phase, the materials are defined and chosen. For the current path, consisting of two ramps and the connecting bar, the copper was chosen. For the two ferromagnetic plates, from ANSYS library a *M3* steel is chosen, having the properties contained in the *emagM3.SI_MPL* file (ANSYS Documentation). The next step in the preprocessor phase is the mesh generation and load application upon the elements (Figure 19). In this application, for modeling the three-dimensional stationary magnetic field a *SOLID97* element is chosen. For the numerical computation of the stationary magnetic field, the model of the DC circuit-breaker together with the boundary volume is discretized in a number of 1268 nodes and 3623 triangular elements (Vîrjoghe, 2004).

In the postprocessing phase is also applied the load on elements and boundary conditions.

The load on elements is represented by the conduction current density. For 3D analysis, a positive value indicates current flowing in the +Z direction in the plan case and the -Z (loop) direction in the asymmetrical case. The current density is directly applied on the finite elements which form the conductors and its value is $125 \cdot 10^6$ A/m². As boundary conditions the Dirichlet condition, $A=0$, is applied.

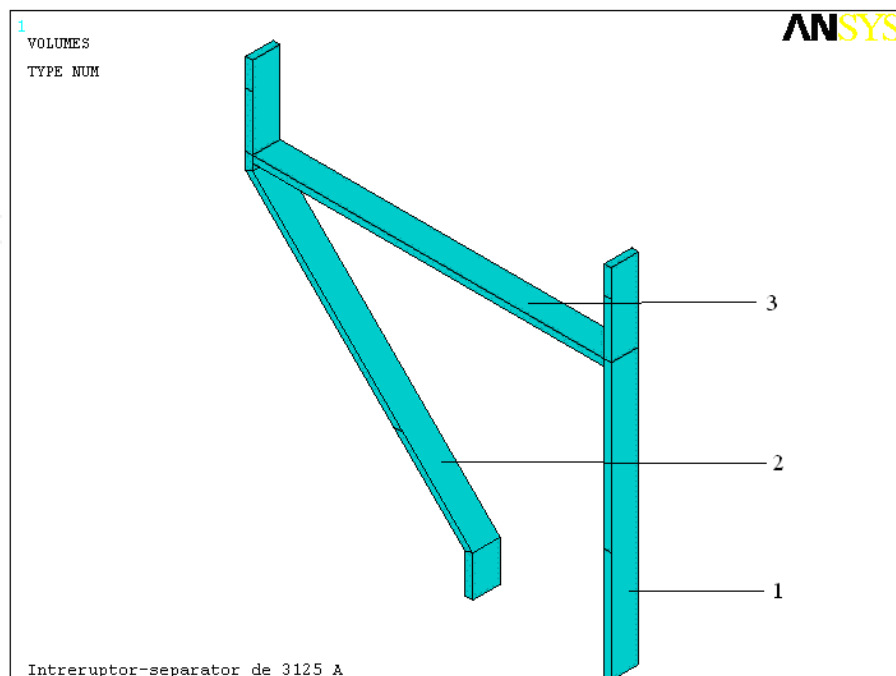


Figure 18. The current path for DC circuit breaker – separator of 3125 A

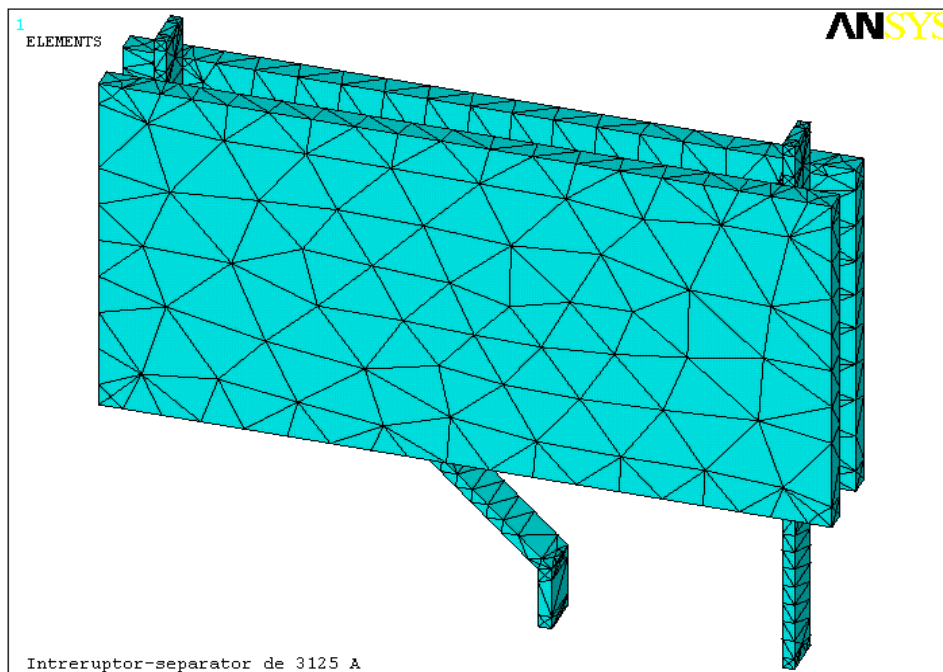


Figure 19. The discretized model of the DC circuit breaker-separator of 3125 A

The Maxwell's equations solver is based on the Finite Element Method (FEM). The results are the nodal values of the primary unknowns (magnetic vector potential) and derivatives of these values for obtaining the secondary unknowns (magnetic induction).

In the postprocessing phase, the tool allows visualization of magnetic induction spectrum, determination of magnetic sizes in arbitrarily chosen points, as well as the evaluation of the different charts. Figure 20 shows the magnetic induction spectrum in the arc-quenching chamber of DC circuit breaker-separator of 3125 A. A maximum value of magnetic induction 2.149 T is obtained.

The DC circuit breaker-separator is designed as a particularly elaborated solution for the current path and the arc-quenching chamber. It is widely known that in electromechanic design of a switching device, the arc-quenching chamber together with current paths and contacts represent the essential element due to their switching performances in normal operating conditions and in abnormal conditions. An optimization criterion of this arc-quenching chamber concerns the ferromagnetic material used in the construction of the ferromagnetic profiles. Simulation was performed for three different steels. For the two ferromagnetic plates, three different steels from ANSYS library are chosen, namely (ANSYS Documentation):

- carpenter (silicon) steel with material properties contained in *emagSilicon.SI_MPL* file;
- iron cobalt vanadium steel with material properties contained in the *emagVanad.SI_MPL* file;
- SA1010 steel with material properties contained in the *emagSa1010.SI_MPL* file.

It was established that in the case of steel EmagSilicon utilization, the maximum value of magnetic induction is 1.883 T, in the case of EmagVanad the maximum value of magnetic induction is 1.975 T and in the case of EmagSa1010 the maximum value of magnetic

induction is 1.44 T. Hence, the optimal material for construction of these profiles is EmagVanad. Although the steel with vanadium is an expensive material, it assures an optimal value of magnetic induction. The high price is compensated by improving the arc-quenching chamber performance and thus increase the breaking capacity of the device (Vîrjoghe, 2004).

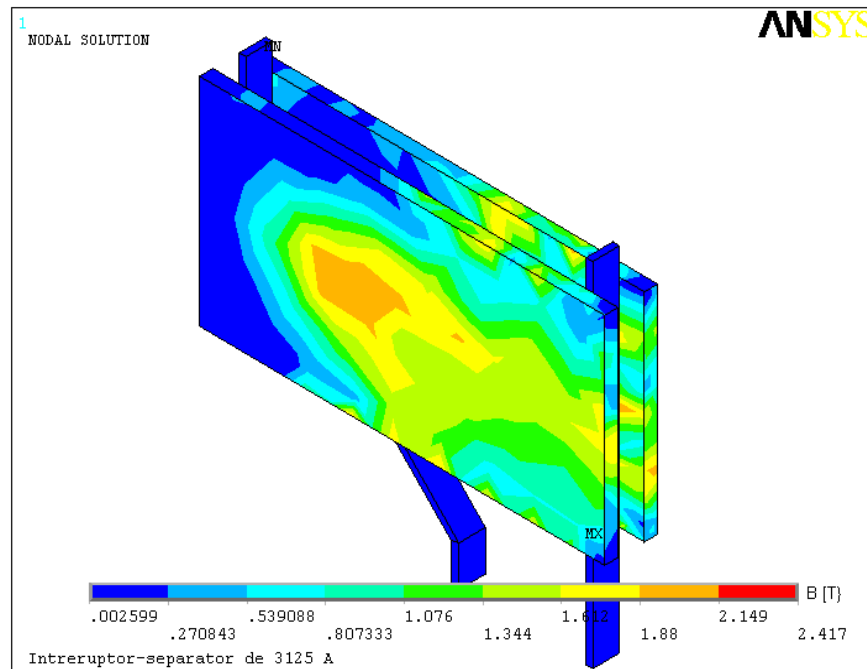


Figure 20. The magnetic induction spectrum in arc-quenching chamber of DC circuit breaker-separator of 3125 A

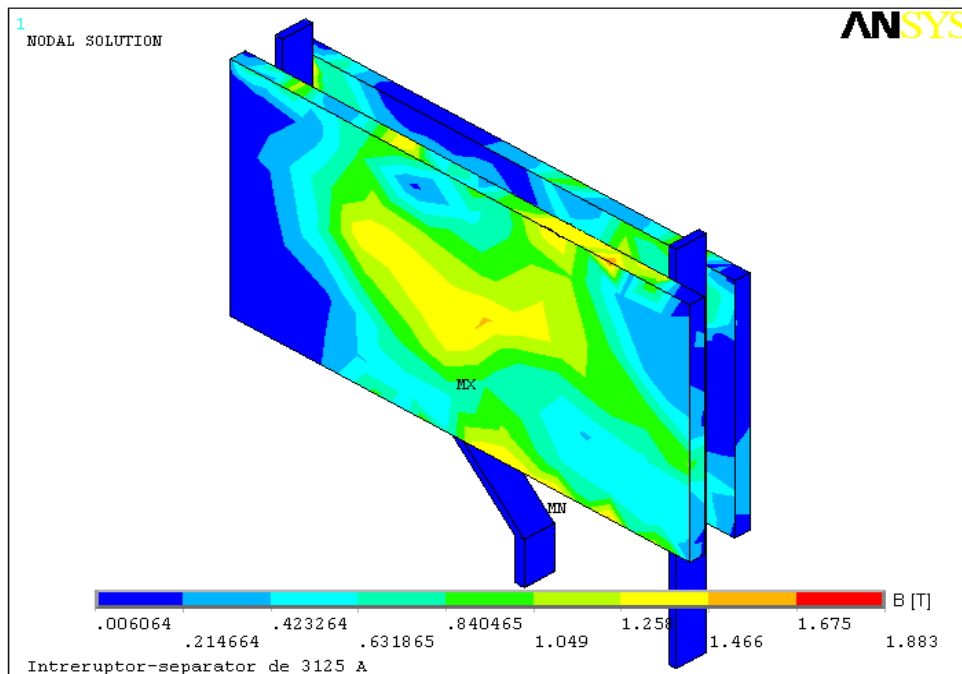


Figure 21. Magnetic induction distribution for the ferromagnetic material EmagSilicon

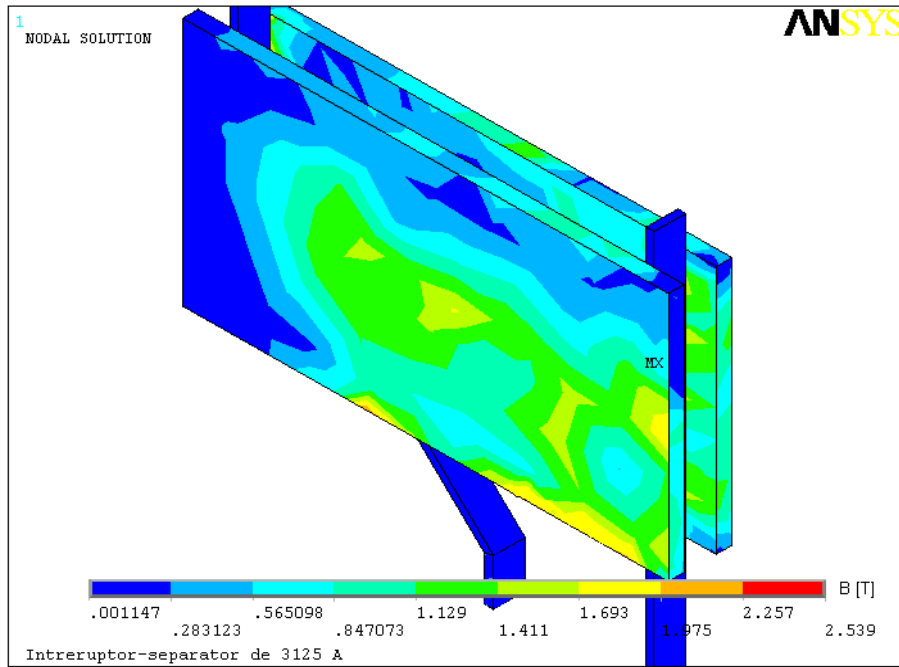


Figure 22. Magnetic induction distribution for the ferromagnetic material EmagVanad

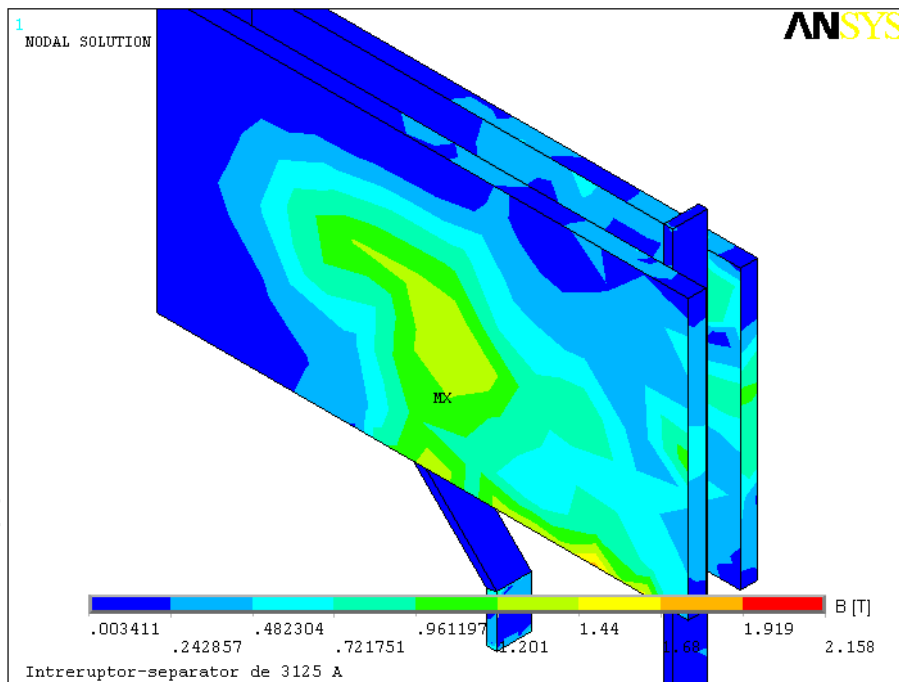


Figure 23. Magnetic induction distribution for the ferromagnetic material EmagSa1010

5. Conclusion

It is well known that in electromechanical construction of a switching device, the arcing chamber along with current paths and contacts represents the all-important elements concerning switching performances of these in normal operating conditions as well as in operation under faults (Trușcă & Trușcă, 2001).

Comparing the magnetic flux density spectrums in the three cases it can be observed that the maximum arc-quenching effect is obtained by using EmagVanad for the ferromagnetic shapes. For this material an optimal distribution for the magnetic field in the circuit breaker arcing chamber is obtained, which leads to a rapid movement of the electric arc towards the ferromagnetic plates. Arc quenching and arc voltage limiting occur in base of the niche effect principle along with the electrode effect (Hortopan, 1996).

Author details

Elena Otilia Virjoghe, Diana Enescu, Mihail-Florin Stan and Marcel Ionel
Valahia University of Targoviste, Romania

6. References

- Andrei, H., Flueraşu, C., Flueraşu, C., Enescu, D., Virjoghe, E.O., Husu, A.G., Andrei, P.C. & Popovici, D. (2012). Metode numerice, modelări și simulări cu aplicații în ingineria electrică/Numerical Methods, Modelling and Simulation Applied in Electrical Engineering, in *Electra*, București, 427-436.
- Eckhardt, H. (1978) Numerische Verfahren in der Energietechnik. Stuttgart:Teubner-Verlag.
- Flueraşu, C., Flueraşu, C. (2007). Electromagnetism, in *Printech*, București.
- Gârbea, D. (1990). Analiză cu elemente finite, in *Tehnică*, București, 7-8.
- Hăntilă, I.F. (2004). Electrotehnica teoretică, in *Electra*, București.
- Hortopan, Gh. (1996). Aparate electrice de comutație, vol.II, in *Tehnică*, București, 58-60.
- Ioan D., Ionescu, B. (1993). Numeric methods in electromagnetic field computation, *Politehnica*, București.
- Mocanu, C.I. (1981). Teoria câmpului electromagnetic, *Didactică și Pedagogică*, București, 456-460.
- Moraru, A. (2002). Bazele electrotehnicii - Teoria câmpului electromagnetic, *MatrixRom*, București.
- Morozionkov, J., Virbalis, J.A. (2008). Investigation of Electric Reactor Magnetic Field using Finite Element Method, *Electronics and Electrical Engineering*, No.5(85).
- Răduleț, R. (1975). Bazele teoretice ale electrotehnicii, Litografia Învățământului, București.
- Silvester P.P., Ferrari, R.L. (1996). Finite Elements for Electrical Engineers, 3rd Edition, *University Press*, Cambridge, 28-29, 118-120, 183-187.
- Șora, C., (1982). Bazele electrotehnicii, *Didactică și Pedagogică*, București, 258-260.
- Stammerger, H. (1995). Magnetfeld-und Kraftberechnungen für strombegrenzende Niederspannungs-Schaltgeräte, *VDI Verlag*, Elektrotechnik, Bonn, pp.12-20.
- Timotin, A., Hortopan, V., Ifrim, A., Preda, V., (1970). Lecții de bazele electrotehnicii, *Didactică și Pedagogică*, București.
- Trușcă, V., Trușcă, B. (2001). Elektrische anlagen – vorlesungen- , *Printech*, Bukarest.
- Virjoghe, E.O., (2004). Aparate electrice de comutație, *Electra*, București, 93-99, 122-129.

Vîrjoghe, E.O., Enescu, D., Ionel, M., Stan, M-F. (2010). 3D Finite Element Analysis for arcing chamber optimization of the current-limiting circuit breaker, *WSEAS TRANSACTIONS on POWER SYSTEMS*, ISSN: 1790-5060, Issue 1, Volume 5.

ANSYS Release 11.0 Documentation.

IntechOpen

IntechOpen